MOLECULAR AND CELLULAR BIOLOGY, Feb. 1995, p. 723–730 Vol. 15, No. 2
0270-7306/95/$04.00+0

AFR1 Promotes Polarized Apical Morphogenesis in *Saccharomyces cerevisiae*

JAMES B. KONOPKA,* CORDELL DEMATTEI, AND COLLEEN DAVIS

Department of Molecular Genetics and Microbiology, State University of New York, Stony Brook, New York 11794-5222

Received 25 July 1994/Returned for modification 15 September 1994/Accepted 2 November 1994

The G protein-coupled α-factor receptor promotes polarized growth toward a mating partner. α-Factor induces the expression of *AFR1*, which acts together with the receptor C terminus to promote normal morphogenesis. The function of *AFR1* was investigated by engineering cells to constitutively express *AFR1* without α-factor. Constitutive *AFR1* expression caused cells to form elongated buds that demonstrate that AFR1 can also interact with the morphogenesis components that promote bud formation. A similar elongated bud phenotype is caused by mutation of the *CDC3*, *CDC10*, *CDC11*, and *CDC12* genes, which encode putative filament proteins that form a ring at the bud neck. AFR1 may act directly on the filament proteins, since immunolocalization detected AFR1 at the bud neck and interaction of AFR1 and CDC12 was detected in the two-hybrid protein assay. AFR1 localized to the base of pheromone-induced projections. These results suggest that AFR1 and the putative filament proteins act together with the receptor to facilitate proper localization of components during mating.

The conjugation of the yeast *Saccharomyces cerevisiae* provides a genetically accessible system for the analysis of hormone-induced cell polarization and morphogenesis. Haploid *S. cerevisiae* cells of opposite mating type, *MAT***a** and *MAT*α (24), signal each other with mating pheromones to undergo conjugation (32, 35, 55). *MAT***a** cells secrete **a**-factor pheromone that activates a receptor on the surface of *MAT*α cells; *MAT*α cells secrete α-factor pheromone that activates a receptor on the surface of *MAT***a** cells. Pheromone receptor signaling stimulates yeast cells to arrest cell division in G_1 and then undergo intracellular reorganization to polarize cell growth toward an appropriate partner cell. The cells then polarize growth toward a gradient of pheromone which enables them to sense the spatial position of an appropriate mating partner (27, 51). Polarized morphogenesis enables pairs of mating cells to make contact and fuse to form zygotes.

The mating-pheromone signal pathway is similar to sensory pathways used in multicellular organisms to detect diverse stimuli such as light, odor, taste, and hormones (15, 23). The α-factor receptor, encoded by *STE2* (6, 42), and the **a**-factor receptor, encoded by *STE3* (21, 42), belong to a large family of receptors that are distinguished by possessing seven transmembrane domains. Biochemical analysis of the most thoroughly studied receptors in this family, the β-adrenergic receptor and rhodopsin, indicates that these receptors transduce their signal by stimulating the α subunit of a heterotrimeric G protein to bind GTP (23). The G_α subunit then dissociates from the $G_{\beta\gamma}$ subunit; either G_α or $G_{\beta\gamma}$ goes on to activate an effector. In *S. cerevisiae*, $G_{\beta\gamma}$ transmits the pheromone signal by activating the subsequent steps in the signaling pathway that include MAP kinase homologs (16). Phosphorylation of a pheromone-responsive transcription factor, STE12, stimulates transcription of genes that function in mating (54). Pheromone signaling stimulates cell division arrest through inactivation of the *CDC28* protein kinase and associated cyclin proteins by transcriptional and posttranscriptional mechanisms (9, 16).

The yeast pheromone receptors play a key role by signaling cell polarization through G protein-dependent and G protein-independent signal pathways (27). Pheromone-induced morphogenesis is mediated by many of the same components that mediate polarized morphogenesis during bud formation (39). Some of these genes encode cytoskeletal elements such as actin, and others encode signal transduction components such as the CDC24 guanine nucleotide exchange factor (56). In some cases, the products of the genes involved in cell polarization show a polarized distribution within the cell themselves. For example, the leading edge of growth in both structures contains actin, SPA2, calmodulin, and CDC42 proteins (2, 5, 53, 57). Pheromone signal transduction components also become polarized, which suggests that this may be part of the signaling mechanism for cell polarization. The α-factor receptors and the *STE6* protein that promotes **a**-factor secretion are localized to the region of pheromone-induced morphogenesis (27, 34). However, it remains to be determined whether polarization of the pheromone signaling components is a cause or a consequence of cell polarization. The mechanisms by which pheromones stimulate polarized growth in *S. cerevisiae* may be conserved in other organisms. Chemokines such as interleukin-8, which stimulate leukocyte chemotaxis, and cyclic AMP, which stimulates *Dictyostelium discoideum* chemotaxis, activate G protein-coupled receptors that promote actin reorganization and cell polarization (13, 36).

Several investigators have suggested that the pheromone receptors may directly determine the region of polarized growth (4, 11, 27, 40). Interestingly, truncation of the cytoplasmic C terminus of the α-factor receptor causes a defect in forming acute projections of pheromone-induced morphogenesis (33). A similar morphogenesis defect was observed in *afr1* mutant cells (31). Genetic evidence indicates that *AFR1* acts in the same pathway as the receptor C terminus to promote pheromone-induced morphogenesis. *AFR1* also acts in conjunction with the C terminus of the α-factor receptor to promote adaptation to α-factor. To better understand how *AFR1* functions to coordinate signal transduction and morphogene-

* Corresponding author. Mailing address: Department of Molecular Genetics and Microbiology, State University of New York, Stony Brook, NY 11794-5222. Phone: (516) 632-8715. Fax: (516) 632-8891. Electronic mail address: konopka@asterix.bio.sunysb.edu.

TABLE 1. Strains used in this study

Strain	Genotype	Source
DJ211-5-3	*MAT***a** *ade2-1^o bar1-1 cry1 his4-580^a leu2 lys2^o trp1^a tyr1^o ura3 SUP4-3^{ts}*	D. Jenness
DJ147-1-2	*MAT***a** *ade2-1^o cry1 his4-580^a leu2 lys2^o trp1^a ura3 SUP4-3^{ts}*	D. Jenness
JKY7441-4-2	*MAT***a** *ade2-1^o bar1-1 cry1 his4-580^a leu2 lys2^o trp1^a ura3 SUP4-3^{ts} ste2-T326*	J. Konopka
JKY7441-4-4	*MAT***a** *ade2-1^o cry1 his4-580^a leu2 lys2^o trp1^a uyr1^o ura3 SUP4-3^{ts} ste2-T326*	J. Konopka
JK26-1	*MAT***a** *ade2-1^o afr*::*URA3 cry1 his4-580^a leu2 lys2^o trp1^a ura3 SUP4-3^{ts}*	J. Konopka
QCY1-9	*MAT***a** *ade2-1^o bar1-1 cry1 his4-580^a leu2 lys2^o trp1^a tyr1^o ura3 SUP4-3^{ts} ste2*::*URA3*	Q. Chen
JKY35	*MAT***a**/*MAT*α *ade2-1^o*/*ade2-1^o cry1*/*cry1 his4-580^a*/*his4-580^a leu2*/*leu2 lys2^o*/*lys2^o trp1^a*/*trp1^a TYR1*/*tyr1^o ura3*/*ura3 SUP4-3^{ts}*/*SUP4-3^{ts} BAR1*/*bar1-1*	J. Konopka
CTY10-5d	*MAT***a** *ade2 trp1-901 leu2-3,112 his3-200 gal4 URA3*::*lexA-lacZ*	R. Sternglanz
JK7434-2	Tetraploid derivative of DJ211-5-3 except *MAT***a**/*MAT***a**/*MAT***a**/*MAT***a** *TYR1*/*tyr1*/*tyr1*/*tyr1 cry1*/*cry1*/*cry1*/*cry1*	J. Konopka

sis, the subcellular localization of AFR1 protein and the effects of constitutive *AFR1* expression were examined. The results suggest that AFR1 promotes pheromone-induced morphogenesis by interacting with a family of putative filament-forming proteins encoded by *CDC3*, *CDC10*, *CDC11*, and *CDC12* that were shown previously to be involved in bud morphogenesis and cytokinesis (18, 20, 22, 29).

MATERIALS AND METHODS

Strains and media. The yeast strains used in this study are described in Table 1. Cells were grown in media described by Sherman (52). Plasmid-containing cells were grown in synthetic medium containing adenine, uracil, and amino acid additives but lacking leucine to select for plasmid maintenance. Plasmids were transformed into yeast strains with lithium acetate (25).

Galactose-regulated expression of *AFR1*. PCR was used to introduce a *Sal*I site 1 bp 5′ to the ATG of *AFR1*. A 2.2-kb *Sal*I-*Bam*HI fragment of *AFR1* was then inserted after the *GAL10* promoter in a modified version of YEp51 (49) to create pJK47. The modified version of YEp51, which was constructed by S. Johnson and B. Byers, contained a galactose-regulated *GAL10* promoter followed by a polylinker region to facilitate ligation of inserts. Cells carrying pJK47 were grown to mid-logarithmic phase in media containing the noninducing carbon source raffinose. Expression of *AFR1* was induced by the addition of 1% galactose to the medium. Cells were fixed with formaldehyde to preserve their morphology and then photographed with Kodak TMAX film and an Olympus BH2 microscope equipped with differential interference (Nomarski) optics.

Antibody production and purification. Anti-AFR1 antibodies were raised in rabbits immunized with a TrpE-AFR1 fusion protein. A 990-bp *Avr*II-*Cla*I fragment containing *AFR1* codons 20 to 350 was fused in frame to the *trpE* gene in pATH3 (30). *Escherichia coli* expression and purification of the TrpE-AFR1 fusion protein were carried out essentially as described previously (30). Rabbits were immunized with the purified fusion protein (Cocalico Biologicals, Reamstown, Pa.). Rabbit serum (5 ml) was purified by adsorption against four nitrocellulose filters each containing the extract of ~10^9 *afr1*::*URA3* cells and 10^9 *trpE*-producing *E. coli* cells. The adsorbed serum was then affinity purified against 2 mg of nitrocellulose-bound TrpE-AFR1 protein essentially as described previously (47). For immunofluorescence analysis, the antibodies were purified further by five serial adsorptions against 10^8 formaldehyde-fixed, glusulase-digested *afr1*::*URA3* cells.

Western immunoblot analysis. Cells were grown to mid-logarithmic phase and then adjusted to 4×10^6 cells per ml. Cells grown in complete medium were induced with pheromone by the addition of α-factor to 10^{-7} M. Cells carrying pJK47 were grown in medium containing raffinose but lacking leucine. Cells were induced by the addition of galactose to a 1% final concentration, and then approximately 2.5×10^8 cells were harvested and lysed by agitation with glass beads in 250 μl of lysis buffer (2% sodium dodecyl sulfate [SDS], 100 mM Tris [pH 7.5]). The extracts were centrifuged for 5 min at 12,000 × *g*, and then 5 μl of extract (5×10^6 cells) was separated by electrophoresis on an SDS–9% polyacrylamide gel. Samples were electrophoretically transferred to nitrocellulose and probed with anti-AFR1 antibodies diluted into a solution of 1% powdered milk in TBS (10 mM Tris [pH 7.5], 150 mM NaCl). The blot was incubated with alkaline phosphatase-conjugated goat anti-rabbit immunoglobulin G and then the AFR1 protein was detected by a colorimetric assay as specified by the manufacturer (Bio-Rad).

Fluorescence microscopy. Formaldehyde-fixed cells were stained with rhodamine-phalloidin (Molecular Probes, Eugene, Oreg.) to detect actin, with Calcofluor (Sigma, St. Louis, Mo.) to detect chitin, and with 4′,6-diamino-2-phenylindole (DAPI; Boehringer Mannheim, Indianapolis, Ind.) to detect DNA essentially as described previously (46, 47). Results obtained with rhodamine-phalloidin, Calcofluor, and DAPI were consistently observed in at least two independent experiments. Cells were prepared for immunofluorescence analysis as previously described (47). Formaldehyde-fixed cells were treated with glusulase and zymolyase to remove the cell wall, attached to glass slides, and treated with cold methanol and acetone. The slides were incubated with mouse monoclonal anti-actin antibody C4 (Boehringer Mannheim) to detect actin or with affinity-purified rabbit anti-AFR1 to detect AFR1. Samples were treated with fluorescein-conjugated secondary antibodies (Cappel) and then observed by fluorescence microscopy. The samples were photographed with Kodak TMAX film and an Olympus BH-2 microscope. Results obtained by immunofluorescence analysis were consistently observed in at least four independent experiments.

Two-hybrid protein assay. The two-hybrid protein analysis was based on the method of Fields and Song (17) as modified to use a *lexA-AFR1* DNA-binding domain fusion to screen a library of yeast genomic sequences fused to the *GAL4* activation domain (3). The *lexA-AFR1* fusion plasmid (pLAF) was constructed by inserting a *Bam*HI site 5′ of the *AFR1* coding sequence so that the *AFR1* gene could be joined in frame with the *lexA* gene in plasmid pBTM116 (3). The production of a *lexA-AFR1* fusion protein was verified by Western immunoblotting (data not shown). A library of yeast genomic sequences fused to the *GAL4* activation domain in plasmid pGAD was provided by S. Fields and P. Bartell (12). A yeast strain (CTY10-5d) containing four *lexA*-binding sites inserted upstream of a *lacZ* reporter gene (obtained from R. Sternglanz) was cotransformed with pLAF and the *GAL4* activation domain library. Transformed colonies were screened for induction of the *lacZ* reporter gene by imprinting the colonies onto filter paper, lysing the cells by incubation in liquid nitrogen, and then incubating the filters with a colorimetric substrate for β-galactosidase (X-Gal [5-bromo-4-chloro-3-indolyl-β-D-galactopyranoside]). Library plasmids that conferred activation of the *lacZ* reporter gene specifically in combination with a *lexA-AFR1* fusion plasmid were recovered into *E. coli*. The identity of the yeast insert was determined by using an oligonucleotide primer corresponding to the *GAL4* activation domain to obtain the DNA sequence across the fusion junction.

RESULTS

Pheromone-induced cell polarization in *afr1* and *ste2-T326* mutants. *S. cerevisiae* cells that are stimulated with a high dose of pheromone arrest cell division in the unbudded G_1 phase and then form acute projections of new cell growth. Previous studies showed that mutation of *AFR1* or truncation of the α-factor pheromone receptor (*ste2-T326*) caused a defect in forming the acute projections (31). Some morphogenesis mutants, such as *bem1*^{s} mutants, are thought to be defective because they fail to polarize actin (11). Therefore, we investigated the localization of actin in *afr1*::*URA3* and *ste2-T326* mutants. Cells were stained with rhodamine-conjugated phalloidin, and the distribution of actin was visualized by fluorescence microscopy. The distribution of actin in 200 cells was analyzed for each cell type. Pheromone-induced wild-type cells showed the expected result (Fig. 1A); at least 97% of the cells showed a highly polarized distribution of actin with cortical dots of actin at the leading edge of growth and actin cables emanating from the tip into the cell body. A polarized distribution of actin was also detected in at least 90% of *afr1* and 70% of *ste2-T326* mutants after pheromone stimulation (Fig. 1B and C). However, actin was not concentrated into an acute projection in the mutant cells. Thus, AFR1 and the C terminus of the α-factor receptor function to organize actin into a tight cluster but are not essential for polarization.

Chitin localization was also examined, since this cell wall

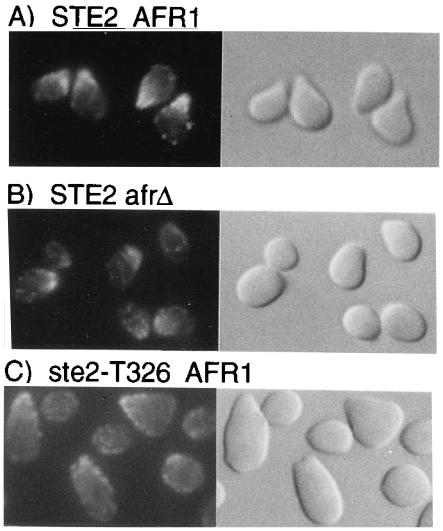

FIG. 1. Actin polarization in α-factor-stimulated cells. Wild-type (A), *afr1*::*URA3* (B), and *ste2-T326 MAT***a** (C) strains were induced with 10^{-7} M α-factor for 90 min and then fixed with formaldehyde. The cells were stained with rhodamine-phalloidin, and then actin localization was detected by fluorescence microscopy. The wild-type (DJ211-5-3), *afr1*::*URA3* (JKY26-1), and *ste2-T326* (JKY7441-4-2) strains are described in Table 1.

component is enriched in the region at the base of pheromone-induced projections (50). This distinct subcellular localization makes chitin a very useful marker for morphological studies. Pheromone-induced cells were stained with Calcofluor and then examined by fluorescence microscopy to visualize chitin. Two hundred cells of each cell type were examined. At least 94% of the wild-type cells showed the expected localization of chitin at the base of the projection but not at the leading edge of growth, where the cortical dots of actin are concentrated (Fig. 2A). In contrast, Calcofluor staining was not uniformly localized in *afr1* or *ste2-T326* cells and many cells varied in

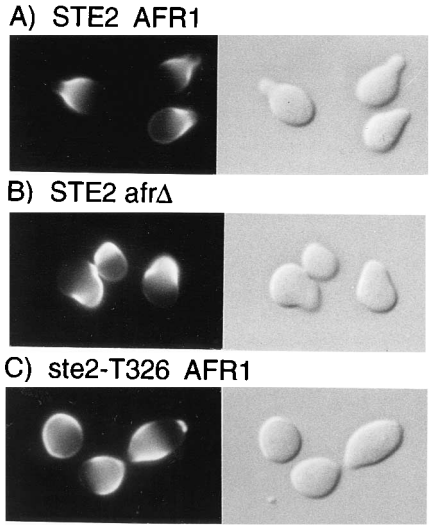

FIG. 2. Chitin polarization in α-factor-stimulated cells. Wild-type (A), *afr1*::*URA3* (B), and *ste2-T326 MAT***a** (C) strains were induced with 10^{-7} M α-factor for 90 min and then fixed with formaldehyde. The cells were stained with Calcofluor to detect cell wall chitin. Calcofluor-stained chitin was detected by fluorescence microscopy. The wild-type (DJ211-5-3), *afr1*::*URA3* (JKY26-1), and *ste2-T326* (JKY7441-4-2) strains are described in Table 1.

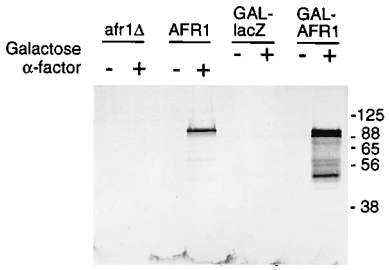

FIG. 3. Western immunoblot analysis of AFR1 protein production. *afr1*::*URA3* cells (JKY26-1) and *AFR1* cells (DJ211-5-3) were induced with α-factor (10^{-7} M) for 90 min. Cells (DJ147-1-2) carrying the vector YEp51 or the GAL10-AFR1 plasmid (pJK47) were induced with galactose for 8 h. Cell extracts were resolved by electrophoresis and transferred to nitrocellulose. The filter was probed with rabbit anti-AFR1 antibodies and then with alkaline phosphatase-conjugated goat anti-rabbit immunoglobulin G. The AFR1 bands were detected by a colorimetric assay for alkaline phosphatase.

staining intensity (Fig. 2B and C). Only 5% of *afr1* and 4% of *ste2-T326* mutants showed the normal staining at the base of a projection. Overall, ≥96% of wild-type cells showed highly polarized chitin staining whereas only 59% of *afr1* and only 15% of *ste2-T326* mutants displayed highly polarized staining. Nonpolarized staining patterns were not due to staining of previous bud sites. Mislocalization of chitin in the *afr1* and *ste2-T326* cells suggests that these cells are defective in localizing other components that are necessary for projection formation.

Immunolocalization of AFR1 protein in α-factor-induced cells. The relationship between actin organization and *AFR1* was analyzed further by immunofluorescence since previous studies showed that actin-binding proteins such as fimbrin and tropomyosin colocalize with actin in vivo (1, 38). Anti-AFR1 antibodies were raised in rabbits (see Materials and Methods), and then the specificity of affinity-purified anti-AFR1 antibodies was tested by Western immunoblot analysis (Fig. 3). A prominent band of approximately 90 kDa was detected in α-factor-induced *AFR1* cells. This band was not detected in extracts from uninduced cells or from cells that lack the *AFR1* gene (*afr1*Δ). α-Factor induction of AFR1 was expected since an *AFR1-lacZ* fusion gene was previously shown to be regulated by α-factor (31). A protein product of similar gel mobility was detected in cells that were engineered to express *AFR1* in response to galactose instead of α-factor. The apparent molecular mass of the AFR1 protein was about 18 kDa larger than the predicted molecular mass of 72 kDa determined from the DNA sequence. The slightly anomalous gel mobility is probably due to the structure of the AFR1 protein and not to post-translational modification, since *E. coli*-produced AFR1 protein showed similar gel mobility (data not shown). These results confirm that the antibodies are specific for the AFR1 protein.

Affinity-purified anti-AFR1 antibodies were used to examine the localization of AFR1 protein in a *MAT***a** tetraploid strain. The increased size of yeast strains with higher ploidy facilitates immunofluorescence analysis (47). Cells incubated without α-factor showed only a low level of background staining (Fig. 4A). α-Factor-induced cells showed staining that was detected primarily at the base of the projection (Fig. 4C and D). More than 90% of the cells were stained by the anti-AFR1 antibody, and nearly all of the cells containing projections showed at least some staining at the base. The AFR1 staining was distinct from actin staining, which was found primarily at the leading edge of the projection (Fig. 4B). Thus, AFR1 does not colocalize with the majority of actin in the cell. AFR1 may be

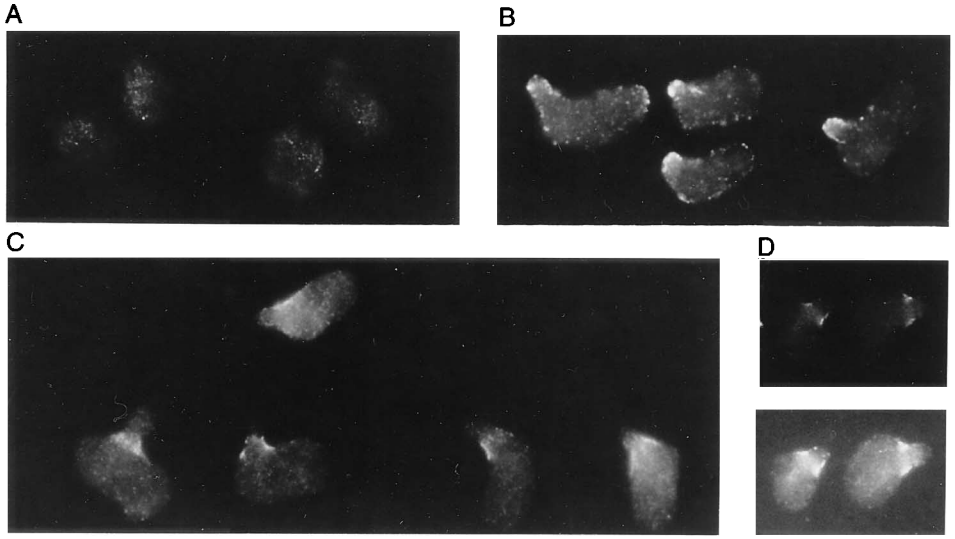

FIG. 4. Immunolocalization of AFR1 in α-factor-induced cells. *MAT***a** strain JK7434-2 was incubated in the absence or presence of α-factor (10^{-7} M) for 120 min. Immunofluorescent staining with affinity-purified anti-AFR1 antibody is shown for cells incubated in the absence (A) or presence (C and D) of α-factor. The upper and lower sections of panel D show a light and dark print of the same cells. Staining with anti-actin monoclonal antibody C4 is shown for cells incubated in the presence of α-factor (B). Fluorescein-conjugated secondary antibodies were used to detect staining with the primary antibody. The cells were prepared for immunofluorescence analysis as described in Materials and Methods.

present in a ring around the base of the projection, since AFR1 staining appears to be concentrated at the edge of the projections (Fig. 4D). AFR1 staining could be detected in the central portion by switching to a new focal plane or by comparison of different photographic prints (Fig. 4D). Similar results were observed for the analysis of chitin, which forms a ring structure in the cell wall around the base of the projection (Fig. 2A).

Morphological effects of constitutive *AFR1* expression. *AFR1* expression is normally regulated by pheromone, so the effects of *AFR1* on cell morphogenesis were examined by engineering constitutive expression of *AFR1* in the absence of pheromone. Inducible *AFR1* expression was engineered by fusing the coding region of *AFR1* to the galactose-inducible *GAL10* promoter as described in the Materials and Methods. The *GAL10-AFR1* gene was inserted into a YEp plasmid vector and then introduced into a *MAT***a** haploid strain for analysis. Galactose induction of *AFR1* resulted in about 50% of cells forming elongated buds (Fig. 5C). The elongated buds were caused by *AFR1* expression, since they were not seen in uninduced cultures (Fig. 5A) or in control cells that were induced with galactose to express *lacZ* instead of *AFR1* (Fig. 5B).

In a previous study, it was observed that α-factor stimulation of *AFR1* expression acted in conjunction with the C terminus of the α-factor receptor to promote projection formation (31). In contrast, galactose induction of *AFR1* promoted the formation of elongated buds in a *ste2-T326* receptor truncation mutant (Fig. 5D). The α-factor receptor itself was not required, since the elongated buds were induced in a *ste2*::*URA3* strain that lacks the receptor gene (Fig. 5E). In fact, none of the haploid-specific mating genes were required since galactose induced the formation of elongated buds in a *MAT***a**/*MAT*α diploid strain (Fig. 5F). These results indicate that in the absence of α-factor-induced cell division arrest, the AFR1 protein alters bud morphogenesis and causes the formation of elongated buds.

Galactose-induced AFR1 protein is concentrated at the bud neck. Immunofluorescence was used to examine the cellular localization of AFR1 protein at various times after induction of the *GAL10-AFR1* gene. Prior to the addition of galactose, the cells showed only a low level of diffuse background staining (Fig. 6A). After 1 h of induction, only about 10% of the cells showed fluorescent staining but, interestingly, the AFR1 staining was concentrated at the neck of the bud (Fig. 6B). By 4 h of induction, at least 80% of the cells showed AFR1 staining throughout the cell (Fig. 6C). However, there was still a concentrated region of staining at the bud neck in the mother cell

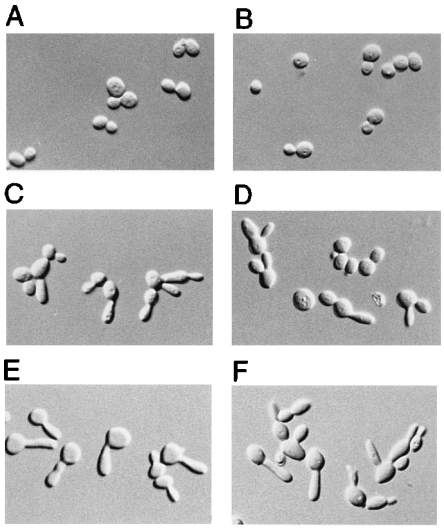

FIG. 5. Morphological effects of galactose-induced *AFR1* expression. Cells carrying a *GAL10-AFR1* plasmid (pJK47) or a control plasmid which contained a *GAL10-lacZ* gene were grown to mid-logarithmic phase, galactose was added to a 1% final concentration to induce gene expression, and the incubation was continued for 4 h at 30°C. (A) Wild-type cells carrying the *GAL10-AFR1* plasmid in the absence of galactose. (B) Wild-type cells carrying a *GAL10-lacZ* plasmid in the presence of galactose. (C to F) Wild-type (C), *ste2-T326* (D), *ste2*::*URA3* (E), and *MAT***a**/*MAT*α (F) cells carrying the *GAL10-AFR1* plasmid induced with galactose. The wild-type (DJ147-1-2), *ste2-T326* (JKY7441-4-4), *ste2*::*URA3* (QCY1-9), and *MAT***a**/*MAT*α (JKY35) strains are described in Table 1.

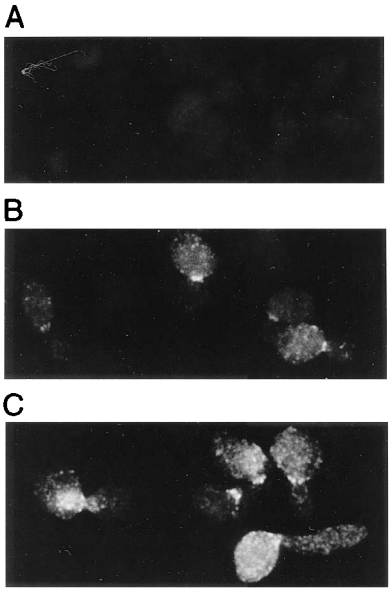

FIG. 6. Immunolocalization of AFR1 in galactose-induced cells. Wild-type cells (DJ147-1-2) carrying a *GAL10-AFR1* plasmid (pJK47) were induced by addition of galactose for 0 min (A), 1 h (B), or 4 h (C). The distribution of AFR1 protein was detected by staining with affinity-purified rabbit anti-AFR1 antibody and with a fluorescein-conjugated goat anti-rabbit immunoglobulin G secondary antibody. Samples were prepared for immunofluorescence analysis as described in Materials and Methods.

in at least 50% of the cells. Thus, AFR1 staining in projections and buds is similar in that staining is not detected at the leading edge of growth but is instead found at the base of the morphogenic structure.

The localization of AFR1 at the bud neck is interesting because the CDC3, CDC10, CDC11, and CDC12 cell division cycle proteins are also located at the bud neck (18, 20, 29). Therefore, the phenotypic effects of constitutive *AFR1* expression were compared with the effects of mutations in *CDC3*, *CDC10*, *CDC11*, or *CDC12*. Temperature-sensitive mutations in *CDC3*, *CDC10*, *CDC11*, or *CDC12* show essentially the same phenotype (22), so only the results for a *cdc3-1*^{ts} strain are presented. Galactose induction of *AFR1* or shifting the *cdc3*^{ts} strain to the nonpermissive temperature both caused the formation of elongated buds (Fig. 7). At later times, some cells started a second bud or a branch off of an existing bud. Examination of the number of nuclei present in each cell by DAPI staining (Fig. 7A and C) showed that nearly all of the large-budded cells were multinucleate. This contrasts with α-factor-induced cells, which arrest in the G_1 phase with a single nucleus. In addition, Calcofluor staining detected the deposition of chitin throughout the cell wall (Fig. 7B and D) in all of the large-budded cells. These similarities in phenotype suggest that the galactose induction of *AFR1* antagonizes the function of *CDC3*, *CDC10*, *CDC11*, and *CDC12*.

AFR1 interacts with CDC12 in the two-hybrid assay. The similar localization of AFR1 and the CDC3, CDC10, CDC11, and CDC12 proteins suggested that they might interact in vivo. This possibility was investigated by a modification of the two-hybrid protein assay developed by Fields and Song (17). In this assay, protein-protein interaction is detected between one protein fused to a DNA-binding domain (LexA) and another protein fused to a transcriptional activation domain (GAL4). Interaction of the hybrid proteins in vivo induces the expression of a *lacZ* reporter gene. Cells carrying a *lexA-AFR1* gene were transformed with a plasmid library of yeast sequences fused to the *GAL4* transcriptional activation domain and were screened for plasmids that activate β-galactosidase production. DNA sequence analysis demonstrated that the *GAL4* activation domain was fused in frame with the *CDC12* gene (Genbank accession number L16551) in two of the six library plasmids that were identified. Both of the *CDC12* isolates contained the same 5′ fusion junction which occurred 18 codons before the putative initiator methionine. The other four library plasmids did not correspond to previously identified genes. The interaction between LexA-AFR1 and GAL4-CDC12 was specific (Fig. 8). The *lexA-AFR1* plasmid did not activate the reporter gene in combination with the *GAL4* activation domain vector; the *lexA* vector or a *lexA-lamin* fusion was not able to activate the reporter in combination with a *GAL4-CDC12* plasmid. These results indicate that AFR1 and CDC12 form a complex that could be due to direct protein

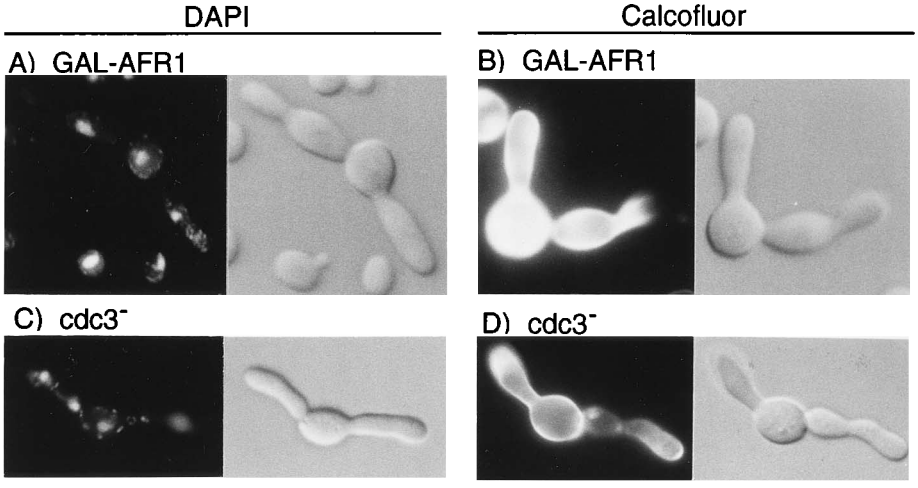

FIG. 7. Phenotypic similarities between cells induced with galactose to express *AFR1* and a *cdc3* mutant. (A and B) Wild-type cells (DJ147-2-1) carrying *GAL10-AFR1* plasmid pJK47 were induced with galactose for 18 h. (C and D) *cdc3*^{ts} mutant cells (H3C1A5) were induced by a shift to the nonpermissive temperature (34°C) for 4 h. The cells were examined by fluorescence microscopy after staining with DAPI to detect DNA and staining with Calcofluor to detect cell wall chitin. A light-microscopic image corresponding to the cells shown in each fluorescent micrograph is shown to the right of each panel.

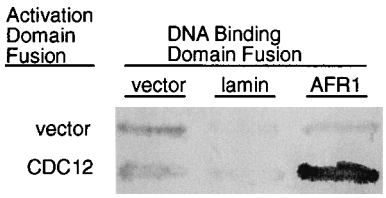

FIG. 8. Interaction of AFR1 and CDC12 in the two-hybrid protein assay. Yeast strain CTY10-5d that carries *lexA*-binding sites upstream of a *lacZ* reporter gene (3) was transformed with the indicated combination of a DNA-binding domain plasmid and transcriptional activation domain plasmid. The DNA-binding domain plasmids expressed either the *lexA* DNA-binding domain alone, a *lexA-lamin* fusion, or a *lexA-AFR1* fusion gene. The activation domain plasmids expressed either the *GAL4* activation domain alone or a *GAL4-AFR1* fusion. Patches of cells were imprinted onto filter paper and then incubated in the presence of a chromogenic substrate for β-galactosidase. A dark patch indicates activation of the *lacZ* reporter gene.

interactions or could be facilitated by a third protein that acts as a bridge. The ability of AFR1 to interact with CDC3, CDC10, and CDC11 in this assay is under investigation.

DISCUSSION

Vegetatively growing yeast cells polarize new growth to create a bud at a predicted site relative to the previous bud site (10). Pheromone stimulation arrests cell division in the unbudded G_1 phase and then polarizes new growth toward a gradient of pheromone (51). This presumably enables yeast cells to effectively discriminate between mating partners (26). The morphological effects of α-factor vary in a dose-dependent manner (41). *MAT***a** cells treated with a low dose of α-factor ($\sim 10^{-9}$ M) form elongated cells. At higher doses of α-factor ($>10^{-8}$ M), polarized growth forms an acute projection. *afr1*Δ mutants and cells producing truncated α-factor receptors (*ste2-T326*) are defective in forming the acute projections normally seen at high concentrations of α-factor. Other mutants that are strongly defective in pheromone-induced morphogenesis, such as *cdc24* and *bem1*, show a defect in cell polarization which is highlighted by a failure to polarize actin (11). In contrast, *afr1*::*URA3* cells and *ste2-T326* mutants showed only a slight defect in actin polarization. Furthermore, *afr1*::*URA3* and *ste2-T326* mutants mate efficiently, which also suggests that they are capable of polarized growth (31). Similar results were reported for *spa2* mutants, which are defective in forming acute projections in response to α-factor and also show only a slight defect in actin polarization and mating (19). These results indicate that *AFR1* and the C terminus of the α-factor receptor act to restrict morphogenesis to a narrow region of the cell but are not essential for cell polarization.

***AFR1* expression promotes apical morphogenesis.** Increased *AFR1* expression correlates with the formation of longer projections: *AFR1* is stimulated in a dose-dependent manner by pheromone, and projections are observed only at high doses of pheromone (31). Furthermore, an increased gene dosage of *AFR1* causes cells to form longer projections in response to α-factor. Therefore, we placed the *AFR1* gene under the control of a galactose-inducible promoter to investigate the effects of *AFR1* on morphogenesis in the absence of α-factor. The results showed remarkable similarity to the effects of *AFR1* expression in pheromone-stimulated cells. Galactose-induced cells formed elongated buds, which indicates that morphogenesis was restricted to a narrow apical region (Fig. 5). In contrast, wild-type cells form round buds because they switch from polarized apical growth to isotropic growth (2, 37).

AFR1 expression affects the type of cell growth that occurs but not the rate of growth. The longer projections and buds take more time to form than do typical projections or buds. The longer projections and buds probably occur because cells maintain polarized apical growth at the same site for a longer period. Thus, *AFR1* expression locks cells into apical morphogenesis and prevents cells from switching to a new morphogenesis site. *AFR1* may act in a positive manner to stabilize an existing site of morphogenesis or in a negative manner to prevent the formation of a new site.

Immunolocalization of AFR1. The subcellular distribution of AFR1 protein was investigated in order to determine whether AFR1 might coincide with the localization of other proteins that function in projection formation, including actin, SPA2, and the α-factor receptors. Actin plays an essential role in polarized yeast morphogenesis by guiding secretory vesicles to dock at a specific site (45). Since *afr1*Δ mutants were defective in restricting actin to an acute projection, it seemed possible that AFR1 acts to bind and organize actin. The function of SPA2 protein is unknown, but it is required for projection formation and is also localized at the tips of projections (19, 53). The C termini of the α-factor receptors, which are detected throughout the projections (27), act in the same genetic pathway as AFR1 to promote projection formation. Surprisingly, AFR1 was detected primarily at the base of the projection and did not colocalize with the majority of actin at the apex (Fig. 3). AFR1 protein could interact with the actin cables that radiate into the cell body, but actin cables are apparently not required for α-factor-induced morphogenesis (48). The distribution of AFR1 also differed from the reported location of SPA2 and the α-factor receptors. However, it is interesting that the location of AFR1 partially overlaps that of the receptors.

The localization of AFR1 to the base of projections is interesting because it coincides with the reported localization of the bud morphogenesis proteins CDC3 and CDC11 (18, 29). The role of CDC3 and CDC11 in projection formation is unknown, but they act together with CDC10 and CDC12 in bud morphogenesis (22). The CDC3, CDC10, CDC11, and CDC12 proteins localize to the neck of the bud, where they appear to form a ring structure (18, 20, 29). Interestingly, AFR1 was detected primarily at the bud neck in cells that were induced with galactose to express *AFR1* (Fig. 6). AFR1 and the CDC proteins could use independent signals to localize to the same sites. However, since AFR1 interacts with CDC12 in the two-hybrid protein assay (Fig. 8), it seems possible that the localization of AFR1 is determined by binding to CDC12. The CDC3, CDC10, CDC11, and CDC12 proteins may also be responsible for the proper localization of other components. They are required for deposition of a ring of chitin in the cell wall at the bud neck and may be needed for the proper localization of components needed for cytokinesis. The cell wall at the base of projections is also enriched in chitin. Interestingly, this chitin is mislocalized in *afr1*::*URA3* and *ste2-T326* mutants (Fig. 2). This suggests that the pheromone receptors, AFR1, and the CDC3, CDC10, CDC11, and CDC12 proteins may mediate the proper localization of other components to the projections.

Mechanism of AFR1 action. α-Factor arrests cell division in the unbudded phase, and then AFR1 acts in a morphogenesis pathway involving the C terminus of the α-factor receptor to promote projection formation. Surprisingly, neither the receptor nor any other haploid cell-specific genes were required to observe the elongated buds that were caused by galactose induction of *AFR1* (Fig. 5). These results indicate that the galactose-induced AFR1 protein manifests its effect by interacting with components of bud morphogenesis. Several lines of evidence suggest that galactose-induced *AFR1* acts in the same

pathway as the *CDC3*, *CDC10*, *CDC11*, and *CDC12* bud morphogenesis genes. The phenotype of cells induced with galactose to express *AFR1* shows striking similarity to the temperature-sensitive phenotype of *cdc3*, *cdc10*, *cdc11*, and *cdc12* mutants. All of these cells form elongated buds that fail to septate, mislocalize chitin, and become multinucleate (Fig. 7). In addition, AFR1 and the CDC3, CDC11, and CDC12 proteins localize to the bud neck in the mother cell. CDC3, CDC10, CDC11, and CDC12 encode a family of homologous proteins that are thought to form a ring of 10-nm filaments in the bud neck (7, 18, 20, 29). This filamentous ring is absent in *cdc3*, *cdc10*, *cdc11*, and *cdc12* mutants (8). Thus, AFR1 may negatively regulate the formation of the filamentous ring or its subsequent function. However, it is premature to conclude that the normal function of AFR1 is to negatively regulate the CDC3, CDC10, CDC11, and CDC12 proteins, since galactose-induced *AFR1* expression is a nonphysiological perturbation.

The results presented in this paper indicate that AFR1 acts in conjunction with the CDC3, CDC10, CDC11, and CDC12 proteins to form projections in pheromone-stimulated cells. The filamentous ring has not yet been observed in pheromone-induced projections, but CDC3 and CDC11 have been detected by immunolocalization in the same region of projections as the AFR1 protein (18, 29). During budding, CDC3, CDC10, CDC11, and CDC12 are thought to act by facilitating the proper localization of components required for cytokinesis. Perhaps the action of these putative filament proteins is modified by AFR1 to promote proper localization of components required for pheromone-induced morphogenesis. It has been proposed that the α-factor-stimulated receptors promote the assembly of an organizing center that is analogous to the bud site (11, 27, 40). This organizing center could include the CDC3, CDC10, CDC11, and CDC12 proteins as well as other components that function in bud and projection formation.

A *Drosophila* homolog of *CDC3*, *CDC10*, *CDC11*, and *CDC12* called *peanut* may also function to localize cellular components (43). *peanut* shows functional similarity to *CDC3*, *CDC10*, *CDC11*, and *CDC12* since it was required for cytokinesis, and the *peanut* protein was localized to cleavage furrows during cytokinesis. Interestingly, *peanut* was isolated as an enhancer of a defect in photoreceptor cell development and the *peanut* protein was detected at the apical surfaces of developing photoreceptors in the eye imaginal disc. Neufeld and Rubin (43) speculate that *peanut* may act to localize molecules, such as signal transduction components, to these domains. It is also interesting that the surface expression of a lymphocyte homing receptor was decreased in mouse cells that express low levels of Diff6, a murine homolog of the yeast filament proteins (44). Additional homologs of the yeast filament proteins have also been found in mice and fungi (14, 28). It will be interesting to determine if homologs of AFR1 participate in the developmentally regulated localization of signal transduction components in other organisms.

ACKNOWLEDGMENTS

We thank S. Fields, R. Sternglanz, and P. Bartell for providing strains and plasmids and for helpful advice on the two-hybrid system. Thanks are also extended to B. Garvick and L. Hartwell for yeast strains and to J. Bliska for a critical reading of the manuscript.

This research is supported by a grant from the American Cancer Society (VM-40). J.B.K. is supported in part by an ACS Junior Faculty Research Award, and C.R.D. is supported by predoctoral training grant 5 T32 CAO 9176-16 from the National Cancer Institute.

REFERENCES

1. **Adams, A. E. M., D. Botstein, and D. G. Drubin.** 1991. Requirement of yeast fimbrin for actin organization and morphogenesis in vivo. Nature (London) **354:**404–408.
2. **Adams, A. E. M., and J. R. Pringle.** 1984. Relationship of actin and tubulin distribution to bud growth in wild-type and morphogenetic-mutant *Saccharomyces cerevisiae*. J. Cell Biol. **98:**934–945.
3. **Bartell, P. L., C.-T. Chien, R. Sternglanz, and R. Fields.** 1993. Using the two-hybrid system to detect protein-protein interaction, p. 153–179. *In* D. A. Hartley (ed.), Cellular interactions in development: a practical approach. Oxford University Press, Oxford.
4. **Bender, A., and G. F. Sprague.** 1989. Pheromones and pheromone receptors are the primary determinants of mating specificity in the yeast *Saccharomyces cerevisiae*. Genetics **121:**463–476.
5. **Brockerhoff, S. E., and T. N. Davis.** 1992. Calmodulin concentrates at regions of cell growth in *Saccharomyces cerevisiae*. J. Cell Biol. **118:**619–629.
6. **Burkholder, A. C., and L. H. Hartwell.** 1985. The yeast α-factor receptor: structural properties deduced from the sequence of the *STE2* gene. Nucleic Acids Res. **13:**8463–8475.
7. **Byers, B., and L. Goetsch.** 1976. A highly ordered ring of membrane-associated filaments in budding yeast. J. Cell Biol. **69:**717–721.
8. **Byers, B., and L. Goetsch.** 1976. Loss of the filamentous ring in cytokinesis—defective mutants of budding yeast. J. Cell Biol. **70:**35a.
9. **Chang, F., and I. Herskowitz.** 1990. Identification of a gene necessary for cell cycle arrest by a negative growth factor of yeast: FAR1 is an inhibitor of a G1 cyclin, CLN2. Cell **63:**999–1011.
10. **Chant, J., and I. Herskowitz.** 1991. Genetic control of bud site selection in yeast by a set of gene products that constitute a morphogenetic pathway. Cell **65:**1203–1212.
11. **Chenevert, J., K. Corrado, J. R. Pringle, and I. Herskowitz.** 1992. A yeast gene (*BEM1*) required for cell polarization whose product contains two SH3 domains. Nature (London) **356:**77–79.
12. **Chien, C.-T., P. L. Bartell, R. Sternglanz, and S. Fields.** 1991. The two-hybrid system: a method to identify proteins encoded by a plasmid library that interact with a protein of interest. Proc. Natl. Acad. Sci. USA **88:**9578–9582.
13. **Devreotes, P. N., and S. H. Zigmond.** 1988. Chemotaxis in eukaryotic cells: a focus on leukocytes and Dictyostelium. Annu. Rev. Cell Biol. **4:**649–686.
14. **DiDomenico, B. J., N. H. Brown, J. Lupisella, J. R. Greene, M. Yanko, and Y. Koltin.** 1994. Homologs of the yeast neck filament associated genes: isolation and sequence analysis of *Candida albicans CDC3* and *CDC10*. Mol. Gen. Genet. **242:**689–698.
15. **Dohlman, H. G., J. Thorner, M. G. Caron, and R. J. Lefkowitz.** 1991. Model systems for the study of 7-transmembrane-segment receptors. Annu. Rev. Biochem. **60:**653–688.
16. **Elion, E. A., J. A. Brill, and G. R. Fink.** 1991. *FUS3* represses *CLN1* and *CLN2* and in concert with *KSS1* promotes signal transduction. Proc. Natl. Acad. Sci. USA **88:**9392–9396.
17. **Fields, S., and O. K. Song.** 1989. A novel genetic system to detect protein-protein interactions. Nature (London) **340:**245–246.
18. **Ford, S. K., and J. R. Pringle.** 1991. Cellular morphogenesis in the *Saccharomyces cerevisiae* cell cycle: localization of the *CDC11* gene product and the timing of events at the budding site. Dev. Genet. **12:**281–292.
19. **Gehrung, S., and M. Snyder.** 1990. The *SPA2* gene of Saccharomyces cerevisiae is important for pheromone-induced morphogenesis and efficient mating. J. Cell Biol. **111:**1451–1464.
20. **Haarer, B. K., and J. R. Pringle.** 1987. Immunofluorescence localization of the *Saccharomyces cerevisiae CDC12* gene product to the vicinity of the 10-nm filaments in the mother-bud neck. Mol. Cell. Biol. **7:**3678–3687.
21. **Hagen, D. C., G. McCaffrey, and G. F. J. Sprague.** 1986. Evidence the yeast *STE3* gene encodes a receptor for the peptide pheromone **a**-factor: gene sequence and implications for the structure of the presumed receptor. Genetics **83:**1418–1422.
22. **Hartwell, L. H.** 1971. Genetic control of the cell division cycle in yeast. Exp. Cell Res. **69:**265–276.
23. **Hepler, J. R., and A. G. Gilman.** 1992. G proteins. Trends Biochem. Sci. **17:**382–387.
24. **Herskowitz, I.** 1989. A regulatory hierarchy for cell specialization in yeast. Nature (London) **342:**749–757.
25. **Ito, H., Y. Kukuda, K. Murate, and A. Kimura.** 1983. Transformation of intact yeast cells treated with alkali cations. J. Bacteriol. **153:**163–168.
26. **Jackson, C. L., and L. H. Hartwell.** 1990. Courtship in *Saccharomyces cerevisiae*: both cell types choose mating partners by responding to the strongest pheromone signal. Cell **63:**1039–1051.
27. **Jackson, C. L., J. B. Konopka, and L. H. Hartwell.** 1991. *S. cerevisiae* α-pheromone receptors activate a novel signal transduction pathway for mating partner discrimination. Cell **67:**389–402.
28. **Kato, K.** 1991. Sequence analysis of twenty mouse brain cDNA clones selected by specific expression patterns. J. Neurosci. **2:**704–711.
29. **Kim, H. B., B. K. Haarer, and J. R. Pringle.** 1991. Cellular morphogenesis in the *Saccharomyces cerevisiae* cell cycle: localization of the *CDC3* gene product and the timing of events at the budding site. J. Cell Biol. **112:**535–544.

30. **Koerner, T. J., J. E. Hill, A. M. Meyers, and A. Tzagaloff.** 1991. High-expression vectors with multiple cloning sites for construction of *trpE* fusion genes: pATH vectors. Methods Enzymol. **194:**477–490.
31. **Konopka, J. B.** 1993. *AFR1* acts in conjunction with the α-factor receptor to promote morphogenesis and adaptation. Mol. Cell. Biol. **13:**6876–6888.
32. **Konopka, J. B., and S. Fields.** 1992. The pheromone signal pathway in Saccharomyces cerevisiae. Antonie Leeuwenhoek **62:**95–108.
33. **Konopka, J. B., D. D. Jenness, and L. H. Hartwell.** 1988. The C terminus of the *Saccharomyces cerevisiae* α-pheromone receptor mediates an adaptive response to pheromone. Cell **54:**609–620.
34. **Kuchler, K., R. E. Sterne, and J. Thorner.** 1989. Saccharomyces cerevisiae *STE6* gene product: a novel pathway for protein export in eukaryotic cells. EMBO J. **8:**3973–3984.
35. **Kurjan, J.** 1992. Pheromone response in yeast. Annu. Rev. Biochem. **61:** 1097–1131.
36. **Lasky, L. A.** 1993. Combinatorial mediators of inflamation? Curr. Biol. **3:**366–368.
37. **Lew, D. J., and S. I. Reed.** 1993. Morphogenesis in the yeast cell cycle: regulation by Cdc28 and cyclins. J. Cell Biol. **120:**1305–1320.
38. **Liu, H., and A. Bretscher.** 1989. Disruption of the single tropomyosin gene in yeast results in the disappearance of actin cables from the cytoskeleton. Cell **57:**233–242.
39. **Madden, K., C. Costigan, and M. Snyder.** 1992. Cell polarity and morphogenesis in *Saccharomyces cerevisiae*. Trends Cell Biol. **2:**22–29.
40. **Madden, K., and M. Snyder.** 1992. Specification of sites for polarized growth in *Saccharomyces cerevisiae* and the influence of external factors on site selection. Mol. Biol. Cell. **3:**1025–1035.
41. **Moore, S. A.** 1983. Comparison of dose-response curves for α-factor-induced cell division arrest, agglutination, and projection formation of yeast cells. J. Biol. Chem. **258:**13849–13856.
42. **Nakayama, N., A. Miyajima, and K. Arai.** 1985. Nucleotide sequences of *STE2* and *STE3*, cell type specific sterile genes from *Saccharomyces cerevisiae*. EMBO J. **4:**2643–2648.
43. **Neufeld, T. P., and G. M. Rubin.** 1994. The Drosophila peanut gene is required for cytokinesis and encodes a protein similar to yeast putative bud neck filament proteins. Cell **77:**371–379.
44. **Nottenburg, C., W. M. Gallatin, and T. St. John.** 1990. Lymphocyte HEV adhesion variants differ in the expression of multiple gene sequences. Gene **95:**279–284.
45. **Novick, P., and D. Botstein.** 1985. Phenotypic analysis of temperature-sensitive yeast actin mutants. Cell **40:**405–516.
46. **Pringle, J. R.** 1991. Staining of bud scars and other cell wall chitin with calcofluor. Methods Enzymol. **194:**732–735.
47. **Pringle, J. R., A. Adams, D. G. Drubin, and B. K. Haarer.** 1991. Immunofluorescence methods for yeast. Methods Enzymol. **194:**565–602.
48. **Read, E. B., H. H. Okamura, and D. G. Drubin.** 1992. Actin- and tubulin-dependent functions during *Saccharomyces cerevisiae* mating projection formation. Mol. Biol. Cell **3:**429–444.
49. **Rose, M. D., and J. R. Broach.** 1991. Cloning genes by complementation in yeast. Methods Enzymol. **194:**195–230.
50. **Scheckman, R., and V. Brawley.** 1979. Localized deposition of chitin on the yeast cell surface in response to mating pheromone. Proc. Natl. Acad. Sci. USA **76:**645–649.
51. **Segall, J. E.** 1993. Polarization of yeast cells in spatial gradients of α-mating factor. Proc. Natl. Acad. Sci. USA **90:**8332–8336.
52. **Sherman, F.** 1991. Getting started with yeast. Methods Enzymol. **194:**3–20.
53. **Snyder, M.** 1989. The *SPA2* protein of yeast localizes to sites of cell growth. J. Cell Biol. **108:**1419–1429.
54. **Song, O., J. Dolan, Y. Yuan, and S. Fields.** 1991. Pheromone-dependent phosphorylation of the yeast *STE12* protein correlates with transcriptional activation. Genes Dev. **5:**741–750.
55. **Sprague, G. F., Jr., and J. W. Thorner.** 1992. Pheromone response and signal transduction during the mating process of *Saccharomyces cerevisiae*: gene expression, p. 657–744. *In* E. W. Jones, J. R. Pringle, and J. R. Broach (ed.), The molecular and cellular biology of the yeast *Saccharomyces*. Cold Spring Harbor Laboratory Press, Cold Spring Harbor, N.Y.
56. **Zheng, Y., R. Cerione, and A. Bender.** 1994. Control of the yeast bud-site assembly GTPase Cdc42. Catalysis of guanine nucleotide exchange by Cdc24 and stimulation of GTPase activity by Bem3. J. Biol. Chem. **269:**2369–2372.
57. **Ziman, M., D. Preuss, J. Mulholland, J. M. O'Brien, D. Botstein, and D. I. Johnson.** 1993. Subcellular localization of Cdc42p, a *Saccharomyces cerevisiae* GTP-binding protein involved in the control of cell polarity. Mol. Biol. Cell **4:**1307–1316.